NJC

Accepted Manuscript

This is an *Accepted Manuscript*, which has been through the Royal Society of Chemistry peer review process and has been accepted for publication.

Accepted Manuscripts are published online shortly after acceptance, before technical editing, formatting and proof reading. Using this free service, authors can make their results available to the community, in citable form, before we publish the edited article. We will replace this *Accepted Manuscript* with the edited and formatted *Advance Article* as soon as it is available.

You can find more information about *Accepted Manuscripts* in the Information for Authors.

Please note that technical editing may introduce minor changes to the text and/or graphics, which may alter content. The journal's standard Terms & Conditions and the Ethical guidelines still apply. In no event shall the Royal Society of Chemistry be held responsible for any errors or omissions in this *Accepted Manuscript* or any consequences arising from the use of any information it contains.

ROYAL SOCIETY OF CHEMISTRY

www.rsc.org/njc

New Journal of Chemistry

ARTICLE

A high selectivity fluorescent chemosensor for cyanide anion based on a chalcone derivative in the present of iron (III) ion, and its capacity for living cell imaging in mixed aqueous system

Received 00th January 20xx,
Accepted 00th January 20xx

DOI: 10.1039/x0xx00000x

www.rsc.org/

Wen Yang[a], Zhongqin Cheng[b], Yunlong Xu[a], Jie Shao[a], Weiqun Zhou[a*], Juan Xie[a], Mengying Li[b*]

*A donor-acceptor chalcone based 4-dimethylamino 4-fluorochalcone (**1**) is found exhibiting a distinct green fluorescence and has a good stability in CH_3CN/water (V/V=1:9) buffer solution (Tris-HCl, pH=7.4), and that the in situ formed **1**-Fe^{3+} complex upon addition of Fe^{3+} serves as a highly selective cyanide anion probe by the turn-on fluorescence performance. Furthermore, the fluorescence imaging experiments of **1**-Fe^{3+} in the present of CN^- in human glioma living cells (U251) demonstrate its potential of practical applications in the biological and environmental systems.*

1 Introduction

Anion recognition is an area of considerable attention in supramolecular chemistry,[1–10] due to the importance of several anions in biological, environmental and chemical processes. Cyanide follows with the most interest among various anions, because it is universally known as one of the most quick-acting and extreme toxicity in physiological and environmental system. For instance, cyanide can binds heme cofactors to inhibit the process of cellular respiration in mammals.[11–16] Also, even very small amounts of the cyanide cause diseases of the vascular, cardiac, visual, endocrine, central nervous and metabolic systems.[17] In addition, some industries such as nylon, acrylic polymers synthesis, electroplating, and gold mining [18] release cyanides to the environment, which cause serious pollution. Therefore, exploring selective and sensitive methods for CN^- detection is very urgent and indispensable.

During the last decades, a number of detecting strategies have been adopted in cyanide recognition by hydrogen bonding interactions,[19] forming complexes,[20] nucleophilic addition to activated carbonyl groups,[21,22] C=C bond[23] and a boron center,[24] and demetalation of preassembled complexed sensor.[25,26] Among these sensing mechanisms, a metal-based receptor is considered to be an ideal approach for CN^- recognition. Up to now, recognition of cyanide by Cu^{2+} displacement approach has been proved to be a valuable method to built highly selective chemosensors for cyanide in aqueous media,[27-30] and can also effectually avoid the interference from other anions such as fluoride and acetate. However, few other metal complexes have been reported for sensing CN^- in aqueous media except for Fe^{3+}. [31]

D-A chalcones, exhibiting intramolecular charge transfer (ICT) fluorescence characteristics, show good photo-physical properties and are applied to fluorescent probe for sensing of metal ions.[23-25,29,32,33] 4-dimethylamino 2, 5-dihydroxy chalcone (DMADHC) has been reported as a sensitive opto-chemical sensor for Fe^{3+} depending on gradually fluorescence quenching.[34] However, the low fluorescence quenching factor (0.2432) and the detection in the organic solvent (DMF) disturbed the application of DMADHC. The deficiency is attributed to the formation of intramolecular hydrogen bond between the phenolic hydroxyl and the keto carbonyl in DMADHC.

In the present work, we chose an excellent donor-acceptor chalcone (1) with 4-dimethylamino as donor and carbonyl as acceptor which has been synthesized.[35-37] In CH_3CN, a fluorescence quenching was observed by the addition of Fe^{3+}, and the quenching ratio reached to 0.996. The in situ formed 1-Fe^{3+} complex was found as a highly selective cyanide probe depending on its fluorescence turn-on performance in CH_3CN/water (V/V=1/9) buffer solution (Tris-HCl, pH=7.4). The fluorescence microscopy experiments also demonstrate that 1-Fe^{3+} can be applied to detect CN^- in living cells. Compared with other reported fluorescent chemosensors, our system shows higher selective and sensitive recognition toward CN^- in CH_3CN/water (V/V=1/9) buffer solution (Tris-HCl, pH=7.4) over a wide range of tested anions through the fluorescence intensity change, blue shift and obvious color change from colorless to yellow, and this chalcone is an simple molecule which is easy to synthesize. To the best of our knowledge, this is the first example of fluorescent sensor based on chalcone-Fe^{3+} complex that allows the selective detection of CN^- in mixed aqueous system.

[a] College of Chemistry & Chemical Engineering and Material Science, Soochow University, 199 Ren'ai Road, Suzhou, People's Republic of China, 215123. Email: wqzhou@suda.edu.cn, Tel: +86-0512-65884827.
[b] School of Biology and Basic Medical Sciences, Soochow University, 199 Ren'ai Road, Suzhou, People's Republic of China, 215123. Email: lmysz@126.com, Tel: +86-0512-65880421.

Electronic Supplementary Information (ESI) available: 2D-NMR spectra of chemosensor 1. See DOI: 10.1039/x0xx00000x

2 Results and discussion

4-dimethylamino 4-fluorochalcone (1) was synthesized according to the references, and 1-Fe^{3+} (100 μmol·L^{-1}) was synthesized by mixing the same volumes and the same concentrations (200 μmol·L^{-1}) of 1, $FeCl_3$ and CH_3CN solution. The optical property and living cell imaging of 1-Fe^{3+} were researched as below.

2.1 The formation of 1-Fe^{3+} in CH_3CN and CH_3CN/water (V/V=1/9) buffer solution (Tris–HCl, pH=7.4)

The fluorescence quantum yield of 1(QY, 0.324) was determined taking quinine sulfate in 0.05 mol·L^{-1} sulfuric acid as the standard. Fig. 1 showed the addition of Fe^{3+} to 1 in CH_3CN caused the fluorescence quenching, and the quenching reached its maximum after the addition of two equivalents of Fe^{3+}. The fluorescence quenching factor, κ ($\Delta F/F_0$) calculated to be 0.996. The QY of 1 in CH_3CN/water (V/V=1/9) buffer (Tris–HCl, pH=7.4) solution was 0.036. The fluorescence quenching factor κ decreased to 0.697 and accompanied with a slight blue shift of the fluorescence maximum emission (from 530 to 513 nm) due to the addition of water.

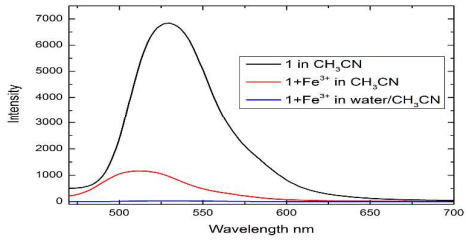

Fig. 1 The fluorescence comparison of 1+Fe^{3+} in CH_3CN and water/CH_3CN

In general, an interested sensor should be suitable to recognize analytes in aqueous system. So, the properties of 1-Fe^{3+} were then studied in CH_3CN/water (V/V=1/9) buffer solution (Tris–HCl, pH=7.4) at 513 nm. As shown in Fig. 2(a), adding two equivalents of Fe^{3+} to 1 also reached its maximum fluorescence quenching. The Job's plot (Fig. 2(b)) showed that the maximum fluorescence quenching was at a molar fraction of 0.5, which indicated that the binding stoichiometry for 1-Fe^{3+} was 1:1.

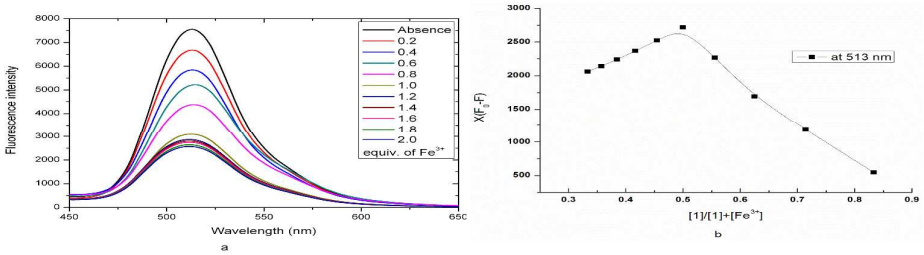

Fig. 2 Fluorescence titration of 1 (10μM) in the presence of various equivalents of Fe^{3+} in CH_3CN/water (V/V=1/9) buffer (Tris–HCl, pH=7.4) solution (a); the stoichiometry analysis of 1-Fe^{3+} by Job's plot analysis (X= [1]/ [1] + [Fe^{3+}]) (b).

2.2 The pH titration

A suitable pH range of 1-Fe^{3+} was conducted to determining fluorescence intensity at 513 nm in the different pH CH_3CN/water (V/V=1/9) solution. Fig. 3 showed that the changes of the fluorescence quenching factors of 1-Fe^{3+} were small at a pH range of 6~8. When the pH was lower than 5, the quenching factor κ decreased dramatically, which was attributed to that the protonation of dimethylamino group hindrances the formation of complex. While the pH >9, the κ decreased also due to the hydrolysis of Fe^{3+}. Thus, the best pH range of 1-Fe^{3+} was approximately 6~8 which is suitable for detecting in biological system.

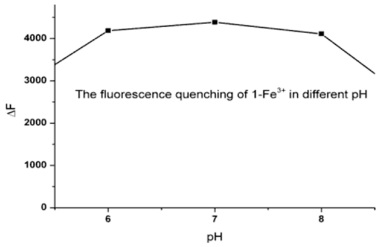

Fig. 3 Fluorescence quenching (ΔF, at 513 nm) of 1 (10μM) after adding 2.0 equivalents Fe^{3+} in different pH values CH_3CN/water (V/V=1/9) buffer (Tris–HCl, pH=7.4) solution.

2.3 Recognition of CN^-

The selectivity of 1-Fe^{3+} complex for CN^- was inspected by the iron-cyanide affinity. The naked-eyes detection carried out by the addition of F^-, Cl^-, Br^-, I^-, Ac^-, CN^-, SO_4^{2-}, $H_2PO_4^-$, HPO_4^{2-}, HCO_3^-, SO_3^{2-}, $HPPi^{3-}$ and Cit^{3-} (2.0 equivalents) in CH_3CN of 1-Fe^{3+} (10 μM) was

depicted in Fig. 4. CN^- was the exclusive one to cause a change in color (from colorless to yellow), while other species such as F^-, Cl^-, Br^-, I^-, Ac^-, SO_4^{2-}, $H_2PO_4^-$, HPO_4^{2-}, HCO_3^-, SO_3^{2-}, $HPPi^{3-}$ and Cit^{3-} demonstrated almost no change in both naked eyed and fluorescence under the identical conditions. CN^- titration against 1-Fe^{3+} was monitored using UV–Vis spectra (Fig.5) in CH_3CN. The UV–Vis spectra showed a gradually increased absorption band at 420 nm (λ_{max}) upon addition of 0.0-2.0 equivalents of CN^-. Another absorption band at 290 nm gradually decreased and disappeared finally with the increase of the concentration of CN^-, which implied that an equilibrium was set up between 1-Fe^{3+} and CN^-.

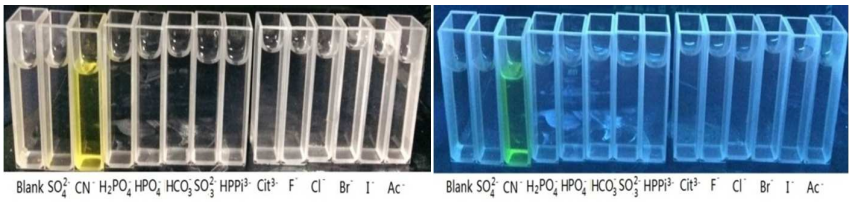

Fig.4 The chromogenic (left) and fluorescence (right) changes of 1-Fe^{3+} (10μM) after addition of various metal ions (20μM) in CH_3CN.

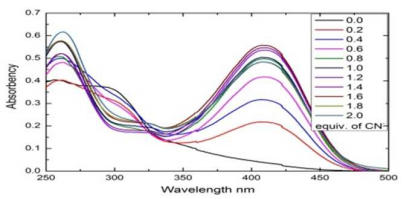

Fig. 5 UV–titration of 1-Fe^{3+} (10μM) to 0-2.0 equivalents CN^- in CH_3CN.

The CH_3CN/water (V/V=1/9) buffer solution (Tris-HCl, pH=7.4) of 1-Fe^{3+} complex (10 μM) was prepared by mixing the solution of 1-Fe^{3+} complex (100 μM) and water (V/V=1/9). The stability of the in situ prepared 1-Fe^{3+} was evaluated further by monitoring the changes of the fluorescence intensity against time (0–60 min) in the CH_3CN/water (V/V=1/9) buffer solution (Tris-HCl, pH=7.4). The fluorescence intensity was almost constant after the addition of Fe^{3+} for 5 min, which indicates the 1-Fe^{3+} has a good stability and suitable for CN^- recognition. Subsequently, the selectivity responses of 1-Fe^{3+} to a variety of anions were investigated (Fig. 6(a)) in the CH_3CN/water (V/V=1/9) buffer solution (Tris-HCl, pH=7.4). Upon addition of 2.0 equiv. of CN^- (Na^+ salt) to the solution of 1-Fe^{3+}, the fluorescence intensity was greatly enhanced. The QY of 1-Fe^{3+}-CN^- was restored to 0.024. However, adding other anions including F^-, Cl^-, Br^-, I^-, Ac^-, SO_4^{2-}, $H_2PO_4^-$, HPO_4^{2-}, HCO_3^-, SO_3^{2-}, $HPPi^{3-}$ and Cit^{3-} (all used as Na^+ salt, 10 equiv. for each) induced negligible fluorescence enhancement. The fluorescence enhancement of 1-Fe^{3+} upon addition of CN^- indicated that the speculated Fe^{3+} displacement approach played a role. It also demonstrated the 1-Fe^{3+} was a good candidate for highly selective recognition of cyanide. The CN^- sensing behavior of 1-Fe^{3+} was also examined by fluorescence titration experiment (Fig. 6(b)). The fluorescence intensity of 1-Fe^{3+} increased upon stepwise adding CN^-, and the fluorescence enhancement reached saturation when 2.0 equiv. of CN^- was introduced. Furthermore, fluorescence competition experiment was conducted to evaluate the tolerance of 1-Fe^{3+} to other anions. As shown in Figure 6(c), the coexistence of equal amount of other anions did not induce any significant interference on the CN^- recognition of 1-Fe^{3+}. These results demonstrated that the CN^- recognition by 1-Fe^{3+} had an excellent anti-jamming ability.

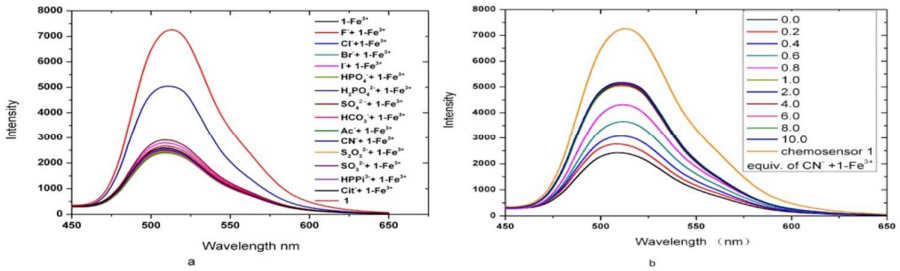

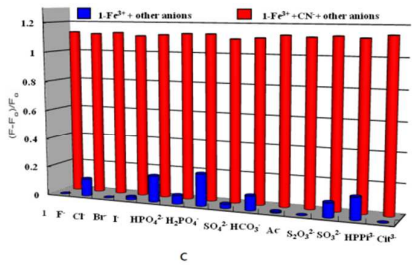

Fig. 6 Fluorescence responses of 1-Fe^{3+} (10μM) to various anions (20μM) in CH_3CN/water (V/V=1/9) buffer (Tris–HCl, pH = 7.4) solution (a); Fluorescence titration of 1-Fe^{3+} (10μM) in the presence of various equivalents of CN^- in CH_3CN/water (V/V=1/9) buffer solution (Tris–HCl, pH=7.4) (b); The fluorescence selectivity of 1-Fe^{3+} (1:1) to CN^- (20μM) or 20μM of other anions (the blue bar portion) and to the mixture of other anions (20μM) (c),The excitation wavelength was 350 nm.

The association constant K_a of 1-Fe^{3+}-CN^- was described in Fig. 7(a). The fitted Benesi–Hildebrand equation was linearized and the obtained association constant K_a for CN^- binding to 1-Fe^{3+} was 2.43 $\times 10^3$. The detection limit obtained from calibration curve (Fig. 7(b)) was also carried out by the abovementioned method and was calculated to be 1.4×10^{-6} M (K = 3, SD=29.2, n=12), which was superior to the standard of good cyanide chemosensors to 20×10^{-6} M.[38]

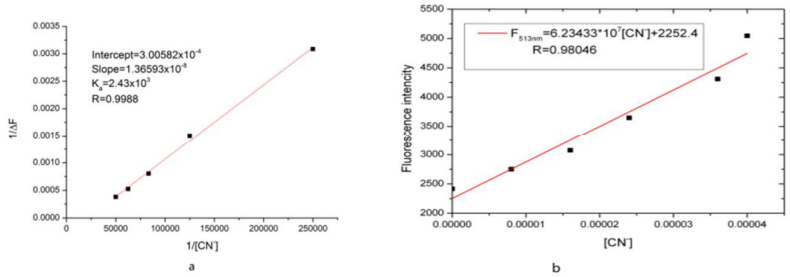

Fig. 7 The Benesi–Hildebrand plot and the calibration curve (b) of 1-Fe^{3+} + CN^- (a) in CH_3CN/water (V/V=1/9) buffer (Tris–HCl, pH=7.4) solution. The monitored wavelength was 513 nm. The excitation wavelength was 350 nm.

2.4 Living cell imaging

To detect CN^- in living cells, U251 cells were cultured in RPMI-1640 supplemented with 6% PBS at 37°C and 5% CO_2. Cells were planted on 15 mm culture dish and allowed to adhere for 48 h. Upon incubation with 20 μM of 1-Fe^{3+} for 30 min at 37°C, the cells displayed a weak intracellular fluorescence image. When further treated with CN^- (40μM) for 10 min in the culture medium, and washed with PBS buffer to remove extracellular CN^-, the bright green fluorescence image enhance gradually in these cells. The fluorescence images were depicted in Fig. 8. The fluorescence and bright-field images revealed that the fluorescence signals were localized in the perinuclear area of the cytosol, indicative of a subcellular distribution due to the high cell membrane permeability of 1-Fe^{3+}.[39-40] These results demonstrated that 1-Fe^{3+} complex was cell membrane permeable and can also be used for imaging of CN^- in living cells and potentially in vivo.

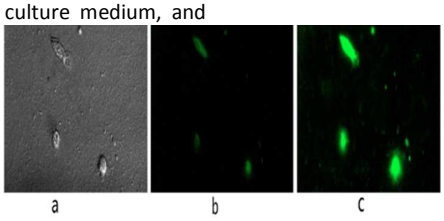

Fig. 8 Fluorescence images of U251 cells treated with 1-Fe^{3+} and CN^-. (a) Bright field image, (b) fluorescence image loaded with 20μM 1-Fe^{3+} for 30 min, (c) fluorescence image of 1-Fe^{3+} loading cells incubated with 50μM NaCN for 30 min.

2.5 Recognition mechanism

The binding mechanism was preliminarily investigated through ^1H NMR. To avoid the effect of the paramagnetism of Fe^{3+}, the testing was carried out with the dilute solution which was made up overnight. In the spectrum of 1 (the signal were amplified), the peak near 6.68 ppm was assigned to the proton signal of H (b) of dimethylamino-phenyl. Addition of Fe^{3+} into the solution led to an apparent downfield shift to 6.92 ppm (2.0 equiv. of Fe^{3+}), which proved the delocalization of dimethylamino-phenyl. The proton signals of H (g) of methyl shifted downfield from 3.02 (absence Fe^{3+}) to 3.13 ppm (2.0 equiv. of Fe^{3+}), which indicated the coordination with Fe^{3+} employed one lone pair of nitrogen of 1. The chemical shifts of H (d) also showed in the lower field (7.31 to 7.38 ppm) upon addition of Fe^{3+}. The downfield sign of H (e) exhibited the trans-configuration of the chalcone double bond. Treatment of the 1-Fe^{3+} system with CN^- afforded a well-resolved spectrum, where the peaks near 6.68 ppm could be found again. The obtained NMR spectrum is similar with that of 1 alone (Fig. 9). These proved that the addition of cyanide ion prompted the dissociation of 1-Fe^{3+} complex and the release of free 1. Based on the fluorescence and NMR spectral evidence as well as reported results, [32] we proposed a possible binding mode as Fig. 10.

New Journal of Chemistry

ARTICLE

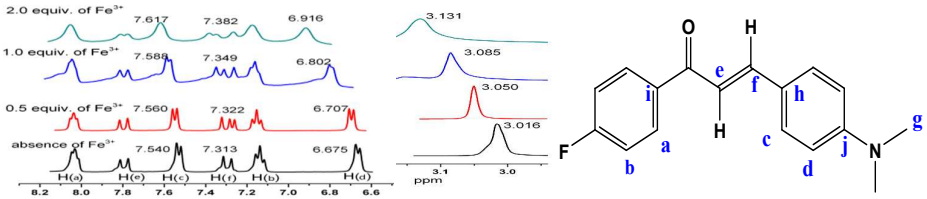

Fig. 9 The ^{1}H NMR spectra of 1 (10μM) in the presence of 0-2.0 equivalent of Fe^{3+} in CD_3CN.

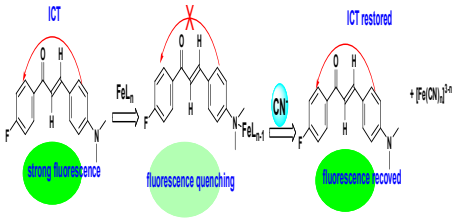

Fig. 10 The proposed sensing mechanism for 1-Fe^{3+} and CN^-

It was worth noting that the addition of CN^- could not regain its initial emission state of 1. This phenomenon might be attributed to the tight binding between 1 and Fe^{3+}, which resulted in incomplete displacement of Fe^{3+} from the complex. To support this recognition mechanism, DFT (B3LYP) calculation at the level of 6-31G (d) was employed. The stable structures and frontier molecular orbital (HOMO and LUMO) of 1-Fe^{3+} and 1 were shown in Figure 11. When 1 coordinated with Fe^{3+} employing a lone electron pair of nitrogen, the excitation of the electron from the highest occupied molecular orbital (HOMO) to the lowest unoccupied molecular orbital (LUMO) populated to Fe^{3+} (Fig. 11(a)). As we known, cyanide ions co-ordinate well to Fe^{3+} ions to form a very stable complex $[Fe(CN)_x]^{3-x}$. When adding CN^- in the solution, the equilibrium of 1-Fe^{3+} + CN^- $\rightleftharpoons$ 1+ $[Fe(CN)_x]^{3-x}$ was set up, and the fluorescence of 1 was exhibited, which indicated a good ICT characteristic. The first excited transition (HOMO → LUMO) of 1 underwent a charge transfer transition from amino-phenyl ring to fluoridephenyl ring (Fig. 11(b)).

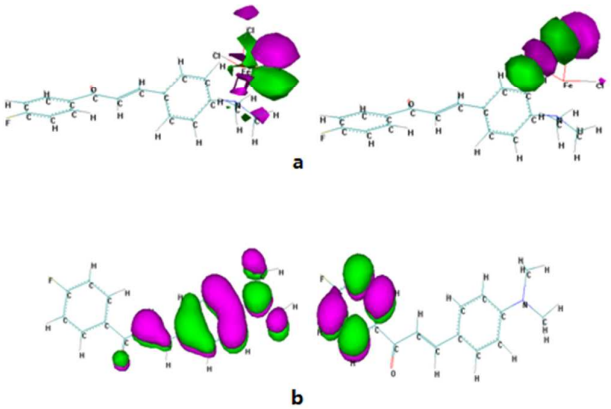

Fig. 11 The optimized structures and the frontier molecular orbital (HOMO (left) and LUMO (right)) of 1-Fe^{3+} (a) and free 1 (b) at the level of B3LYP/6-31G (d).

3 Conclusions

We have successfully designed and synthesized a structurally simple chalcone derivative 1 as a chemosensor for recognition of CN^- in CH_3CN/water (V/V=1/9) buffer solution (Tris-HCl, pH=7.4). The complex 1-Fe^{3+} exhibits high selectivity to cyanide over other anions through fluorescence enhancement. 1-Fe^{3+} also has the significant stability at pH values ranging from 6.0 to 8.0. The association constant K_a of 1-Fe^{3+}-CN^- was 2.43×10^3. The detection limit was calculated to be 1.4×10^{-6} M, which was superior to the standard of good cyanide chemosensors to 20×10^{-6} M. Furthermore, 1-Fe^{3+} shows good cell-permeable and distinct green fluorescence to determine CN^- in living cells of U251. The chemosensor may be found its potential applications in environmental and biological systems. The investigation of binding mechanism indicated that iron ion could coordinate with the N atom of **1** and the stoichiometry of 1-Fe^{3+} was 1:1, which was consistent with the fluorescent experimental results.

4 Experimental

4.1 Reagents

4-fluoroacetophenone, 4-dimethylamino-benzaldehyde, HCl, CD_3CN, NaOH, NaF, NaCl, NaBr, NaI, NaCN, Na_2HPO_4, NaH_2PO_4, Na_2SO_4, $NaHCO_3$, NaAc, Na_2SO_3, Na_3HPPi (Trisodium pyrophosphate) and Na_3Cit (Sodium citrate) were purchased from *J&K* (CHINA). Fe^{3+} was provided by $FeCl_3$. CH_3CN was used as HPLC grade purchased from COSMOSIL (CHINA).

The testing solutions were prepared and measured at room temperature. A stock solution of 1-Fe^{3+} (100 μM) in CH_3CN was diluted to the concentration (10 μM) in CH_3CN/water (V/V=1/9) with Tris–HCl buffer (10 mM, pH=7.4) solution as the determined solution. The fluorescence quantum yield (QY) was determined taking quinine sulfate in 0.05 mol·L^{-1} sulfuric acid as the standard.

4.2 Apparatus

Melting points were determined on a Kofler melting point apparatus and uncorrected. IR spectra were obtained in KBr discs using a Nicolet 170SX FT-IR spectrometer. ^{1}H NMR (400.13MHz) and ^{13}C NMR (101MHz) spectra were recorded by an INOVA 400. TMS (tetramethylsilane) was used as an internal standard for ^{1}H NMR and solvent peak was used as an internal standard for ^{13}C NMR. Elemental analyses were performed on a Yannaco CHNSO Corder MT-3 analyzer. Mass spectra were recorded on a Finnigan MAT95 mass spectrometer (ESI^+). Absorption and fluorescence spectra were recorded on a CARY50 UV-VIS spectrophotometer and an FLS920 fluorescence spectrophotometer. Measurement of pH was performed using a REX PHS-3c acidmeter (INESA Instrument, CHINA). Fluorescent pictures were taken on a Cell'R Live Cell Imaging System (Japan, Olympus).

4.3 Synthesis of 1 and 1-Fe^{3+}

4-fluoroacetophenone, NaOH and 4-dimethylamino-benzaldehyde were grinded in mortar for several minute (4~8 min). On completion of grinding as monitored by TLC (Thin Layer Chromatography), the mixture was diluted with cold water, neutralized by dilute HCl and recrystallized by ethanol.[41-42]

Characterization: Elemental analysis for $C_{17}H_{16}FNO$, Found (%C, H and N): 75.85, 5.93 and 5.22; Stoichiometric amounts (%C, H and N): 75.82, 5.99 and 5.20. FTIR (cm^{-1}): 2902 (ν_{Ph-H}), 2806 (ν_{CH3}), 1647 ($\nu_{C=O}$), 1595 ($\nu_{C=C}$), 1527 (ν_{Ph}), 1412 (ν_{CH3}), 1370 (ν_{CN}), 1226 (ν_{C-C}), 894 (ν_{Ph-H}), 834 (ν_{CH3}), 745 ($\nu_{C=C}$). ^{1}H NMR (CD_3CN) (ppm): 3.016 (s, 6H(g)), 6.656~6.675 (d, 2H(d), J=7.6 Hz), 7.117~7.158 (t, 2H(b), J=8.8 Hz, 8.0 Hz), 7.275~7.314 (d, 1H(e), J=15.6 Hz), 7.520~7.540 (d, 2H(d), J=8.0 Hz), 7.774~7.812 (d, 1H(e), J=15.2 Hz), 8.021~8.054 (t, 2H(a), J=6.4 Hz, 6.8 Hz).^{13}C NMR (CD_3CN) (ppm): 39.976 (C(g)), 111.663 (C(d)), 115.260 (C(b)), 122.289 (C(f)), 130.387 (C(c)), 132.457 (C(a)), 135.231 (C(h)), 145.946 (C(e)), 151.936 (C(j)), 166.627 (C(F)), 188.752 (C(C=O)). The assignment was based on 2D-NMR (Figure S1).

1-Fe^{3+} (100 μmol·L^{-1}) was synthesized by mixing the same volumes and the same concentrations (200 μmol·L^{-1}) of 1, $FeCl_3$ and CH_3CN solution. HRMS (ESI, Figure S2) calc. for $(M + H^+)^+$ 325.85, found 325.97.

4.4 The association constant

The fluorescence intensity at 513 nm was plotted against the molar fraction of 1-Fe^{3+} with 0-2.0 equivalents of CN^-. The association constant (K_a) of 1-Fe^{3+} + CN^- is determined by the Benesi–Hildebrand Eq. (1):[43]

$$\frac{1}{F-F_0}=\frac{1}{\{K_a\times(F_{max}-F_0)\times[CN^-]\}}+\frac{1}{F_{max}-F_0} \quad (1)$$

Where F is the fluorescence intensity at 513 nm at any given CN^- concentration, F_0 is the fluorescence intensity in the absence of CN^-, and F_{max} is the maxima fluorescence intensity at 513 nm in the presence of CN^- in solution. The association constant K_a was evaluated graphically by plotting 1/ ($F-F_0$) against 1/ [CN^-]. Data were linearly fitted according to Eq. (1) and the K_a value was obtained from the slope and intercept of the line. The detection limit (DL) of CN^- was determined from the following equation: DL = K × SD/S,[44] where K = 3, SD is the standard deviation of the blank solution, and S is the slope of the calibration curve.

4.5 Cell culture and fluorescence imaging

U251 cells were purchased by the Shanghai Institute of Cell Biology. The cells were cultured in Roswell Park Memorial Institute culture medium (RPMI-1640), supplemented with 6% calf serum, penicillin (100U·mL^{-1}), streptomycin (100×10^{-6}g·mL^{-1}) and 2.5×10^{-4} M l-glutamine at 37℃ in a 5:95 CO_2–air incubator. The cells were cultured in a 15 mm diameter cell culture dish for 2 days. U251 cells were incubated with a solution of 1-Fe^{3+} (10μM) for 0.5 h, washed three times with phosphate-buffered saline (PBS) buffer solution (pH=7.4), and emission was collected at 525 nm (λ_{ex}=385 nm). Then, further treated with NaCN (50μM) for 10 min in the culture medium, and washed with PBS buffer solution (pH=7.4) to remove

extracellular. All of the images were gathered at the same Live Cell Imaging System and processed with Nikon AY software.

4.6 Theoretical Calculations

Geometry optimization were carried out using DFT (B3LYP)[45-47]method of the Gaussian 09[48] software package with 6-31G (d) basis sets. The calculated harmonic vibration frequencies confirm the stability of the structures.

Acknowledgements

We gratefully acknowledge the financial support of the National Natural Science Foundation of China (No. 51079094) and the Natural Science Foundation of Jiangsu Province (No. BK2010215). The Project was funded by the Priority Academic Program Development of Jiangsu Higher Education Institutions.

Notes and references

1 A. Bianchi, K. Bowman, E. Garcia-Espana, *Supramolecular Chemistry of Anions*, Wiley-VCH, NewYork, 1997.
2 P. D. Beer, P. A. Gale, *Angew.Chem.,* 2001,**113**, 502–532.
3 P. A. Gale (Ed.), *Coord. Chem. Rev.,* 2003, **240**, 1-2.
4 Y. K. Tsui, S. Devaraj, Y. P. Yen, *Sens. Actuators B: Chem.,* 2012, **161**, 510–519.
5 Y. J. Kim, H. K wak, S. J. Lee, J. S. Lee, H. J. Kwon, S. H. Nam, K. Lee, C. Kim, *Tetrahedron,* 2006, **62**, 9635–9640.
6 J. J. Park, Y.H. Kim, C. Kim, J. Kang, *Tetrahedron Lett.,* 2011, **52**, 2759–2763.
7 J. Kang, Y. J. Lee, S. K. Lee, J. H. Lee, J. H. Lee, J. J. Park, Y. Kim, S. J. Kim, C. Kim, *Supramol. Chem.,* 2010, **22**, 267–273.
8 R. M. F. Batista, S. P. G. Costa, M. M. M. Raposo, *Sens. Actuators B: Chem.,* 2014, **191**, 791–799.
9 E. J. Song, H. Kim, I. H. Hwang, K. B. Kim, A. R. Kim, I. Noh, C. Kim, *Sens. Actuators B: Chem.*, 2014, **195**, 36–43.
10 R. Bhattacharya, S. J. S. *Flora, Handbook of Toxicology of Chemical Warfare Agents*, Academic Press, San Diego, 2009, pp. 255–270.
11 L.Tang, P. Zhou, K. Zhong, S. Hou, *Sens. Actuators B: Chem.,* 2013, **182**, 439–445.
12 Y. J. Hyun, J. P. Gyeong, J. N. Yu, W. Ch.Ye, R. Y. Ga, K. Cheal, *Dyes Pigm.*, 2014, **109**, 127-134.
13 B.Vennesland, E. Comm, C. J. Knownles, J. Westly, F. Wissing, *Cyanide in Biology*, Academic Press, London, 1981.
14 Y.L. Wei, G.J. Qin, W.Y. Wang, W. Bian, S.M. Shuang, C. Dong, *J. Lumin.*, 2011, **131**, 1672-1676.
15 K.W. Kulig, *Cyanide Toxicity*, U. S. Department of Health and Human Services, Atlanta, GA, 1991.
16 R. Bhattacharya, S.J.S. Flora, *Handbook of Toxicology of Chemical Warfare Agents,* Academic Press: Boston, 2009, pp 255-270.
17 C. Baird, M. Cann, *Environmental Chemistry*, Freeman, New York, 2005.
18 C. Young, L. Tidwell, C. Anderson, *Minerals, Metals, and Materials Society,* Warrendale, 2001.
19 M. Gaber, T.A. Fayed, S.A. El-Daly, Y.S. El-Sayed, *Photoch. Photobio. Sci.*, 2008, **7**, 257-262.
20 N. DiCesare, J.R. Lakowicz, *Tetrahedron Lett.,* 2002, **43**, 2615-2618.
21 Y. Sato, M. Morimoto, H. Segawa, T. Shimidzu, *J. Phys. Chem.,* 1995, **99**, 35-39.
22 Z.P. Liu, X.Q. Wang, Z.H. Yang, W.J. He, *J. Org. Chem.* 2011, **76**, 10286-10290.
23 A.O. Doroshenko, A.V. Grigorovich, E.A. Posokhov, V.G. Pivovarenko, A.P. Demchenko, *Mol. Eng.*, 1999, **8**, 199-215.
24 N. Marcotte, S. Fery-Forgues, D. Lavabre, S. Marguet, V.G. Pivovarenko, *J. Phys. Chem. A,* 1999, **103**, 3163-3170.
25 T.A. Fayed, *Chem. Phys.,* 2006, **324**, 631-638.
26 F. Wang, L. Wang, X.Q. Chen, J.Y. Yoon, *Chem. Soc. Rev.* 2014, **43,** 4312-4324.
27 Z.C Xu, J. Pan, R. David, J.N. Cui , J.Y. Yoon, *Tetrahedron,* 2010, **66**, 1678-1683.
28 L.J. Tang, N.N. Wang, Q. Zhang, J.J. Guo, R. Nandhakumar, *Tetrahedron Lett.*, 2013, **54**, 536-540.
29 L.J. Tang, M.J. Cai, *Sens. Actuators B: Chem.,* 2012, **173**, 862-867.
30 H.Y. Jo, G.J. Park, Y.J. Na, Y.W. Choi, G.R. You, C. Kim, *Dyes Pigm.*, 2014, **109**, 127 – 134.
31 Z.Q. Hu, M. Du, L.F. Zhang, F.Y. Guo, M.D. Liu, M. Li, *Sens. Actuators B: Chem.,* 2014, **192**, 439– 443.
32 M.W. Hentze, M.U. Muckenthaler, B. Galy, C. Camaschella, *Cell*, 2010, **142**, 24-38.
33 K. Rurack, J.L. Bricks, G. Reck, R. Radeglia, U. Resch-Genger, *J. Phys. Chem. A*, 2000, **104**, 3087-3109.
34 Y.L. Wei, G.J. Qin, W.Y. Wang, W. Bian, S.M. Shuang, C. Dong, *J. Lumin.,* 2011, **131**, 1672-1676.
35 S.B. Bole, L.V.G. Nargund, L.N. Sachindra, K.S. Devaraju, S.D. Shruthi, *Res. J. Pharm., Biol. Chem. Sci.,* 2011, **2**, 119-127.
36 L. V. G. Nargund, V. Hariprasad, G. R. N. Reddy, *Indian J. Pharm. Sci.,* 1993, **55**, 1-5.
37 S.B. Bole, L.V.G. Nargund, L.N. Sachindra, *J. Ultra Chem.,* 2010, **6**, 303-306.
38 R.P. Daniel, *J. Chem. Educ.,* 2004, **81**, 1345-1347.
39 S.B. Zangade, S. Mokle, A. Vibhute, Vibhute Y, *Chem. Sci. J.,* 2011, CSJ-13.
40 H.A. Benesi, J.H. Hildebrand, J. A. C. S. 1949, **71**, 2703-2707.
41 R. Yang, W.B. Wu, W.Y. Wang, Z. Li, J.G. Qin, *Macromol. Chem. Phys.,* 2010, **211**, 18–26.
42 D.P. Murale, A.P. Singh, J. Lavoie, H. Liew, J. Cho, H.I. Lee, Y.H. Suh, D.G. Churchill, *Sens. Actuators B: Chem.*, 2013, **185**, 755-761.
43 J. Cao, C.C. Zhao, X.Z. Wang, Y.F. Zhang, W.H. Zhu, *Chem. Comm.*, 2012, **48**, 9897-9899.
44 S.R. Liu, S.P. Wu, *Sens. Actuators B: Chem.*, 2012, **171-172**, 1110-1116.
45 T.S. Zwier, *Annu. Rev. Phys. Chem.*, 1996, 47, 205-241.
46 A. Southern, D.H. Levy, G.M. Florio, *J. Phys. Chem. A*, 2003, **107**, 4032-4040.
47 J.R. Clarkson, E. Baquero, V.A. Shubert, E.M. Myshakin, K.D. Jordan, T.S. Zwier, *Science,* 2005, **307**, 1443-1446.
48 M.J. Frisch, G.W. Trucks, H.B. Schlegel, G.E. Scuseria, M.A. Robb, J.R. Cheeseman, G. Scalmani, V. Barone, B. Mennucci, G.A. Petersson, H. Nakatsuji, M. Caricato, X. Li, H.P. Hratchian, A.F. Izmaylov, J. Bloino, G. Zheng, J.L. Sonnenberg, M. Hada, M. Ehara, K. Toyota, R. Fukuda, J. Hasegawa, M. Ishida, T. Nakajima, Y. Honda, O. Kitao, H. Nakai, T. Vreven, J.E. Montgomery, J.A. Peralta Jr, F. Ogliaro, M. Bearpark, J.J. Heyd, E. Brothers, K.N. Kudin, V.N. Staroverov, R. Kobayashi, J. Normand, K. Raghavachari, A. Rendell, J.C. Burant, S.S. Iyengar, J. Tomasi, M. Cossi, N. Rega, J.M. Millam, M. Klene, J.E. Knox, J.B. Cross, V. Bakken, C. Adamo, J. Jaramillo, R. Gomperts, R.E. Stratmann, O. Yazyev, A.J. Austin, R. Cammi, C. Pomelli, J.W. Ochterski, R.L. Martin, K. Morokuma, V.G.Zakrzewski, G.A. Voth, P. Salvador, J.J. Dannenberg, S. Dapprich, A.D. Daniels, O. Farkas, J.B. Foresman, J.V. Ortiz, J. Cioslowski, D.J. Fox, *Gaussian 09*, Gaussian, Inc., Wallingford CT, 2009.

Figure caption:

Fig. 1 The fluorescence comparison of 1+Fe^{3+} in CH_3CN and water/CH_3CN

Fig. 2 Fluorescence titration of 1 (10μM) in the presence of various equivalents of Fe^{3+} in CH_3CN/water (V/V=1/9) buffer (Tris–HCl, pH=7.4) solution (a); the stoichiometry analysis of 1-Fe^{3+} by Job's plot analysis (X= [1]/ [1] + [Fe^{3+}]) (b).

Fig. 3 Fluorescence quenching (ΔF, at 513 nm) of 1 (10μM) after adding 2.0 equivalents Fe^{3+} in different pH values CH_3CN/water (V/V=1/9) buffer (Tris–HCl, pH=7.4) solution.

Fig.4 The chromogenic (top) and fluorescence (bottom) changes of 1-Fe^{3+} (10μM) after addition of various metal ions (20μM) in CH_3CN.

Fig. 5 UV–titration of 1-Fe^{3+} (10μM) to 0-2.0 equivalents CN^- in CH_3CN.

Fig. 6 Fluorescence responses of 1-Fe^{3+} (10μM) to various anions (20μM) in CH_3CN/water (V/V=1/9) buffer (Tris–HCl, pH = 7.4) solution (a); Fluorescence titration of 1-Fe^{3+} (10μM) in the presence of various equivalents of CN^- in CH_3CN/water (V/V=1/9) buffer solution (Tris–HCl, pH=7.4) (b); The fluorescence selectivity of 1-Fe^{3+} (1:1) to CN^- (20μM) or 20μM of other anions (the blue bar portion) and to the mixture of other anions (20μM) (c),The excitation wavelength was 350 nm.

Fig. 7 The Benesi–Hildebrand plot and the calibration curve (b) of 1-Fe^{3+} + CN^- (a) in CH_3CN/water (V/V=1/9) buffer (Tris–HCl, pH=7.4) solution. The monitored wavelength was 513 nm. The excitation wavelength was 350 nm.

Fig. 8 Fluorescence images of U251 cells treated with 1-Fe^{3+} and CN^-. (a) Bright field image, (b) fluorescence image loaded with 20μM 1-Fe^{3+} for 30 min, (c) fluorescence image of 1-Fe^{3+} loading cells incubated with 50μM NaCN for 30 min.

Fig. 9 The ^1H NMR spectra of 1 (10μM) in the presence of 0-2.0 equivalent of Fe^{3+} in CD_3CN.

Fig. 10 The proposed sensing mechanism for 1-Fe^{3+} and CN^-.

Fig. 11 The optimized structures and the frontier molecular orbital (HOMO (left) and LUMO (right)) of 1-Fe^{3+} (a) and free 1 (b) at the level of B3LYP/6-31G (d).

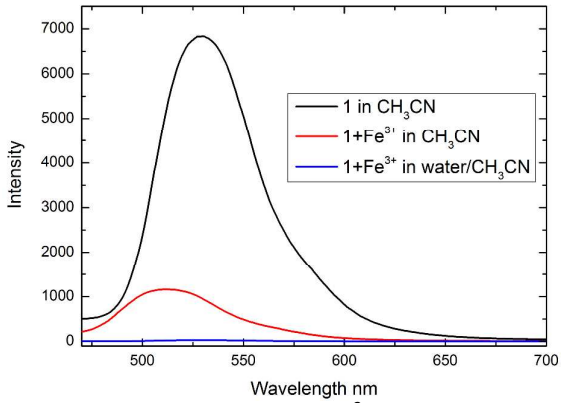

Fig. 1 The fluorescence comparison of $1+Fe^{3+}$ in CH_3CN and water/CH_3CN

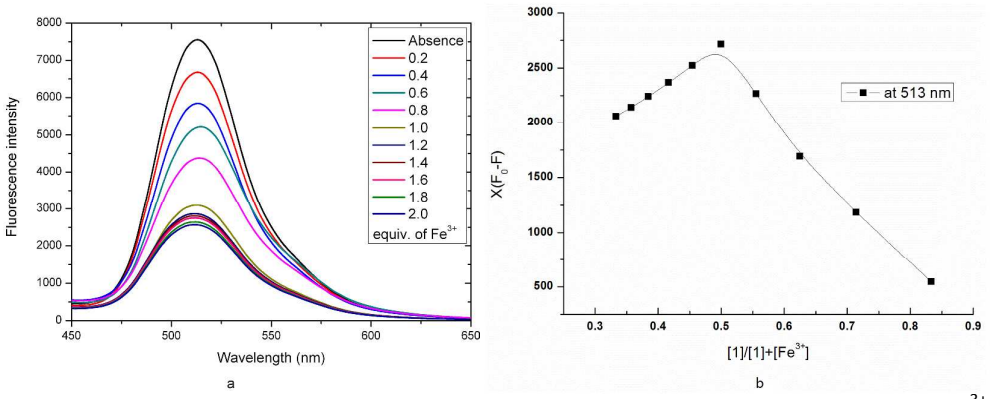

Fig. 2 Fluorescence titration of 1 (10μM) in the presence of various equivalents of Fe^{3+} in CH_3CN/water (V/V=1/9) buffer (Tris–HCl, pH=7.4) solution (a); the stoichiometry analysis of 1-Fe^{3+} by Job's plot analysis (X= [1]/ [1] + [Fe^{3+}]) (b).

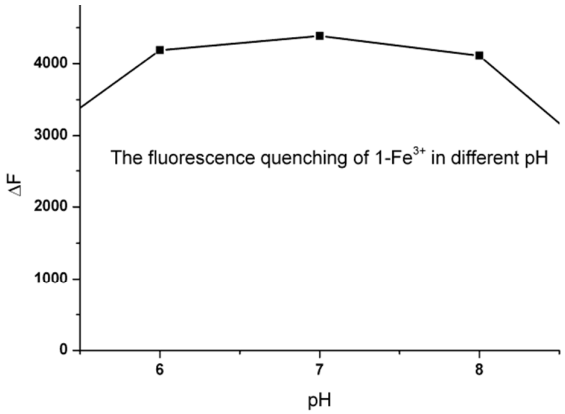

Fig. 3 Fluorescence quenching (ΔF, at 513 nm) of 1 (10μM) after adding 2.0 equivalents Fe^{3+} in different pH values CH_3CN/water (V/V=1/9) buffer (Tris–HCl, pH=7.4) solution.

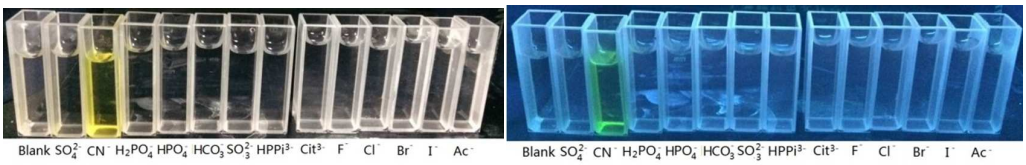

Fig.4 The chromogenic (left) and fluorescence (right) changes of 1-Fe^{3+} (10μM) after addition of various metal ions (20μM) in CH_3CN.

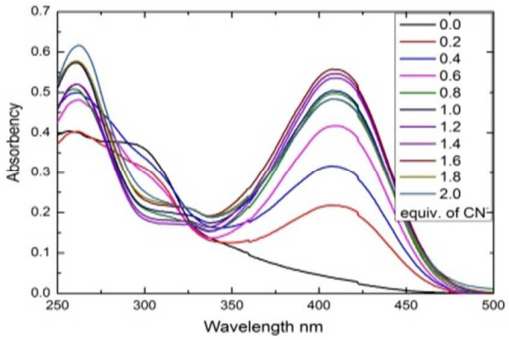

Fig. 5 UV–titration of 1-Fe^{3+} (10μM) to 0-2.0 equivalents CN^- in CH_3CN.

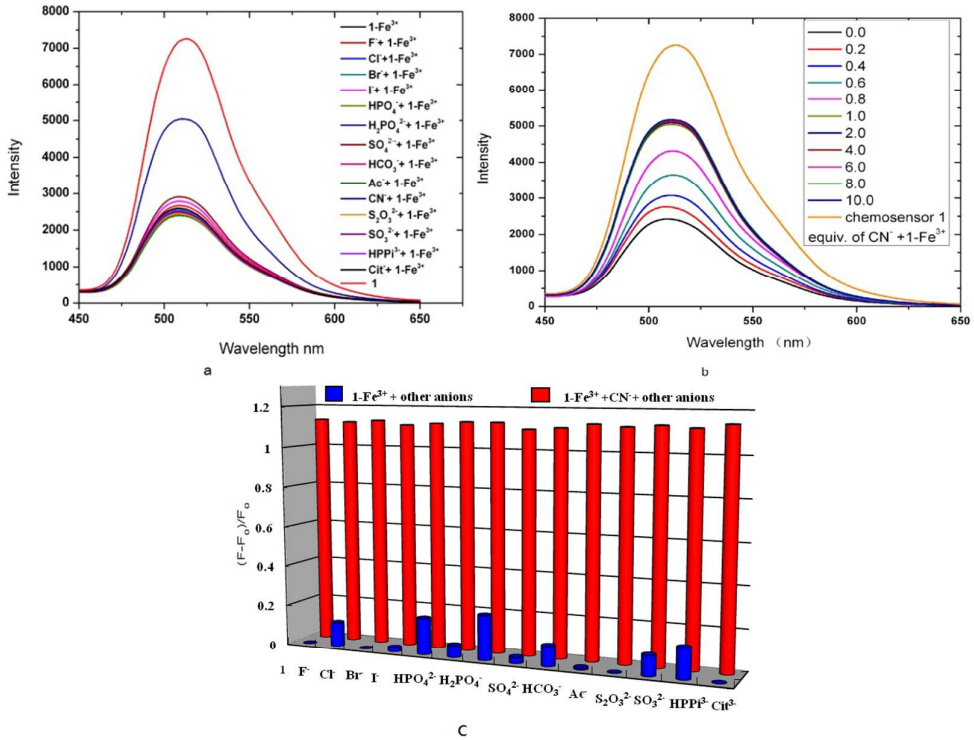

Fig. 6 Fluorescence responses of 1-Fe^{3+} (10μM) to various anions (20μM) in CH_3CN/water (V/V=1/9) buffer (Tris–HCl, pH = 7.4) solution (a); Fluorescence titration of 1-Fe^{3+} (10μM) in the presence of various equivalents of CN^- in CH_3CN/water (V/V=1/9) buffer solution (Tris–HCl, pH=7.4) (b); The fluorescence selectivity of 1-Fe^{3+} (1:1) to CN^- (20μM) or 20μM of other anions (the blue bar portion) and to the mixture of other anions (20μM) (c),The excitation wavelength was 350 nm.

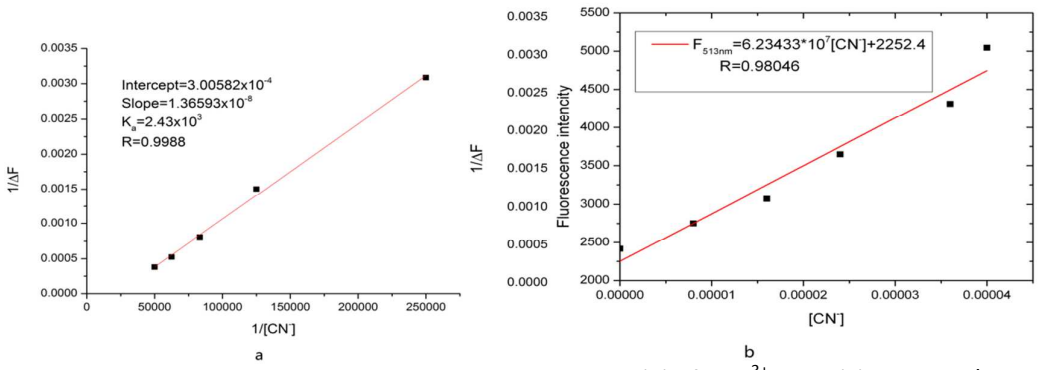

Fig. 7 The Benesi–Hildebrand plot and the calibration curve (b) of 1-Fe^{3+} + CN^- (a) in CH_3CN/water (V/V=1/9) buffer (Tris–HCl, pH=7.4) solution. The monitored wavelength was 513 nm. The excitation wavelength was 350 nm.

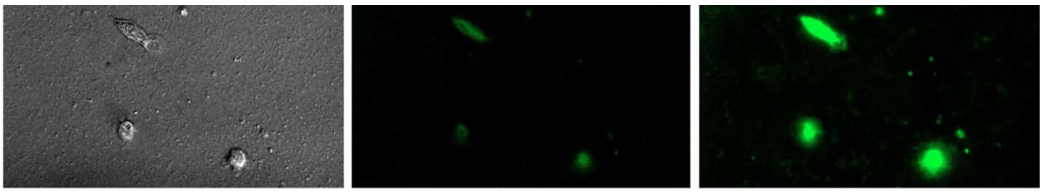

Fig. 8 Fluorescence images of U251 cells treated with 1-Fe^{3+} and CN^-. (a) Bright field image, (b) fluorescence image loaded with 20μM 1-Fe^{3+} for 30 min, (c) fluorescence image of 1-Fe^{3+} loading cells incubated with 50μM NaCN for 30 min.

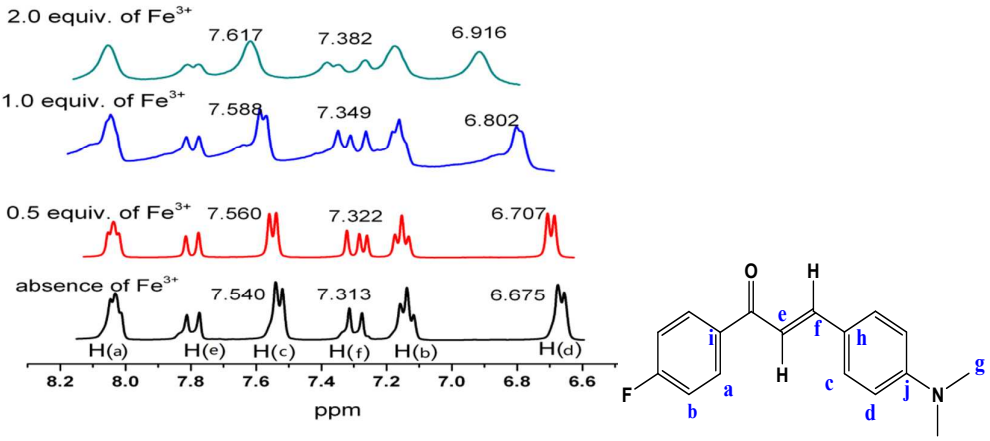

Fig. 9 The ^{1}H NMR spectra of 1 (10μM) in the presence of 0-2.0 equivalent of Fe^{3+} in CD_3CN.

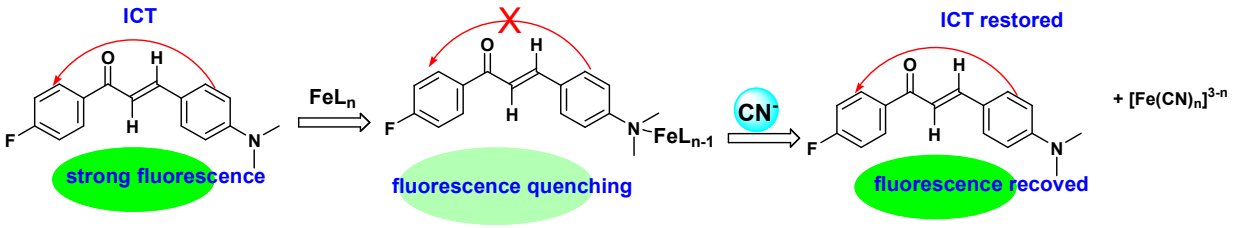

Fig. 10 The proposed sensing mechanism for 1-Fe^{3+} and CN^-.

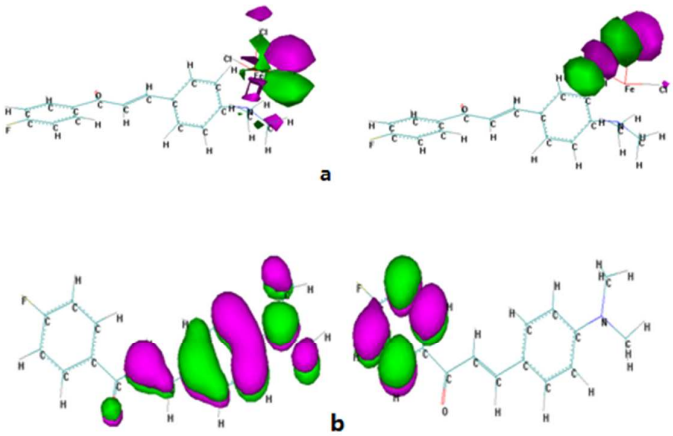

Fig. 11 The optimized structures and the frontier molecular orbital (HOMO (left) and LUMO (right)) of 1-Fe^{3+} (a) and free 1 (b) at the level of B3LYP/6-31G (d).